Available online at www.sciencedirect.com
ScienceDirect
Journal of Power Sources 158 (2006) 1004–1011
JOURNAL OF POWER SOURCES
www.elsevier.com/locate/jpowsour

Thermal analysis of lead-acid battery pastes and active materials

M. Matrakova, D. Pavlov *

Institute of Electrochemistry and Energy Systems (CLEPS), Bulgarian Academy of Sciences, Sofia 1113, Bulgaria

Available online 13 December 2005

Abstract

Thermal methods, differential scanning calorimetry (DSC) and thermogravimetry (TG), are highly sensitive analytical techniques that can be used for quality control of the materials and the technological processes during battery manufacture. This paper presents the results of our investigation aimed to estimate the efficiency of the two thermal methods, differential scanning calorimetry and thermogravimetry, for analysis and control of the processes taking place during battery production and operation.

Keywords: Lead-acid battery; Lead-acid battery technology; Differential scanning calorimetry; Thermogravimetry

1. Introduction

Thermogravimetric analysis (TGA) is a technique, which measures the mass of substances as a function of temperature increase. Differential scanning calorimetry (DSC) is a analytical method by which the difference in energy inputs into a substance and a reference material is measured as a function of temperature, whilst the substance and reference material are subjected to a controlled temperature programme [1].

Thermoanalytical techniques were used by Liptay [2] to investigate the manufacture of active materials for lead-acid batteries, by Corino et al. [3] to determine the percentage of free lead in leady oxide, and by Mawston et al. [4] to characterize active materials for lead-acid batteries, etc.

The aim of our investigation is to estimate the efficiency of the methods of differential scanning calorimetry and thermogravimetry for investigation and control of the processes taking place during battery production and operation.

2. Experimental

2.1. Investigated products

The following materials were investigated: leady oxide, PE separators, Vanisperse A (Borregaard LignoTech), Indulin (MeadWestvaco), as well as chemical products lead hydrocarbonate (Merck) and β-PbO_2 (Merck). The cured pastes and active materials were produced in this laboratory.

2.2. Thermal analysis

All tests were performed using instruments supplied by Mettler Toledo: DSC 822e and TGA/SDTA851e. All measurements were carried out in nitrogen atmosphere at a gas flow-rate of 80 $cm^3\ min^{-1}$ for DSC and 50 $cm^3\ min^{-1}$ for TGA, and at constant heating rate of 10 $K\ min^{-1}$. All materials were dried at 60 °C to evaporate the surface absorbed water. Pure substances and starting materials were investigated with no pretreatment of the samples.

3. Experimental results and discussion

3.1. DSC analysis of leady oxide

The leady oxide is a basic starting material for the production of lead-acid battery plates. The DSC technique is able to measure the free lead content in the sample, irrespective of its particle size, shape and degree of encapsulation by the oxides. Fig. 1a presents the DSC curve for fresh commercial leady oxide. The curve features only a sharp endothermic peak at 328 °C due to metallic lead melting. The measured enthalpy versus the enthalpy on melting of 1 g lead gives the content of lead in the leady oxide in percents. For our leady oxide it was 16.7%. This value is equal to the value determined by chemical wet analysis. However, the DSC measurement takes only about 10 min.

* Corresponding author. Tel.: +359 2 9710083; fax: +359 2 8731552.
E-mail address: dpavlov@labatscience.com (D. Pavlov).

0378-7753/$ – see front matter © 2005 Elsevier B.V. All rights reserved.
doi:10.1016/j.jpowsour.2005.11.007

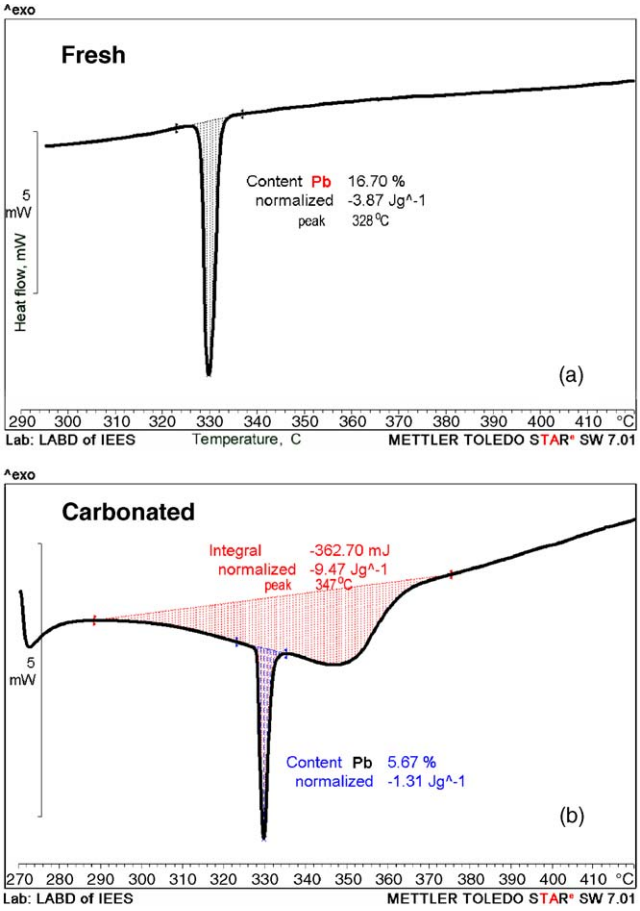

Fig. 1. DSC curves for fresh leady oxide (a) and carbonated leady oxide (b).

The composition of leady oxide can change during storage at room temperature because it reacts with atmospheric CO_2. Fig. 1b presents the DSC curve for the carbonated leady oxide. The curve features, beside the melting peak at 328 °C also a broad endothermic peak from 280 to 375 °C, which results from the degradation of the carbonate formed in the leady oxide. The content of unoxidized lead for carbonated leady oxide is 5.67%. During storage, a great part of lead in leady oxide is oxidized and PbO is partly carbonated.

3.2. DSC curves for Vanisperse A and cured negative paste

Fig. 2 presents the DSC curves for Vanisperse A (pure substance) and for two cured negative pastes with different content of the same expander. The endothermic peak at 130 °C is related to the dehydration of the pure Vanisperse A substance, while the exothermic peak between 350 and 420 °C is a result of expander degradation. Using the measured quantity of energy at the exothermic peak, we can determine the amount of unchanged expander in the cured negative pastes. The inset in the figure shows parts of DSC curves for the negative cured pastes, from 350 to 420 °C, which result from the decomposition of the expander. During paste preparation and curing of the negative plates, part of the expander contained in them disintegrates. The upper curve evidences that 0.26%, of the originally introduced

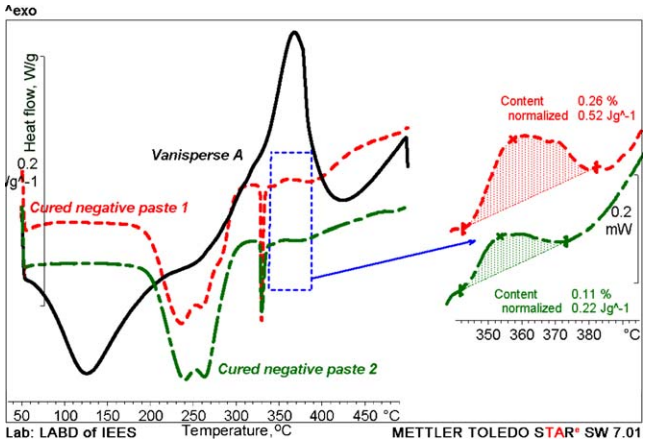

Fig. 2. DSC curves for Vanisperse A and cured negative pastes.

0.50%, expander remains unchanged in the cured paste, whereas in the lower curve the content of unchanged expander is 0.11% against the introduced 0.35%.

The DSC technique allows to determine the similarities in nature between different expander products. Fig. 3 shows DSC and TG curves for Indulin (Kraft pine lignin) and Cedar lignin. It can be seen from the DSC curves that both compounds have the same nature. Judging by the TG curves it can be concluded that Cedar lignin decomposes more readily than Indulin. At $T = 500$ °C, Cedar lignin disintegrates completely even in the absence of oxygen.

3.3. Changes in the polyethylene separator during battery operation

Fig. 4 shows the DSC curves for polyethylene separator before battery assembly and after 150 charge/discharge cycles. The endothermic peak at 130 °C corresponds to the "crystallite melting point". The peak area can be used to determine the proportion between the crystalline and amorphous parts in the separator, which affect the mechanical properties of polyethylene. During battery cycling, flows of H^+, SO_4^{2-} and HSO_4^- ions, and H_2O pass through the separator. Beside the melting peak at 130 °C, a new peak appears at 200 °C in the curve for PE separator after battery cycling. The DSC method offers new possibilities for estimating the changes in composition and structure of the polyethylene separator during battery operation and for evaluation of the current state of health of the separator.

3.4. DSC and TG data for 3BS pastes

Fig. 5 presents DSC curves for commercial 3BS product and for cured 3BS paste. Only one endothermic peak is observed in the curve for the commercial substance at 240 °C. The DSC curve for the cured 3BS paste features an additional endothermic peak at 270 °C. Most probably, beside the crystalline water in the structure of $3PbO{\cdot}PbSO_4{\cdot}H_2O$ there is also another type of bonded water in the 3BS cured paste, which leaves the 3BS particles at higher temperatures.

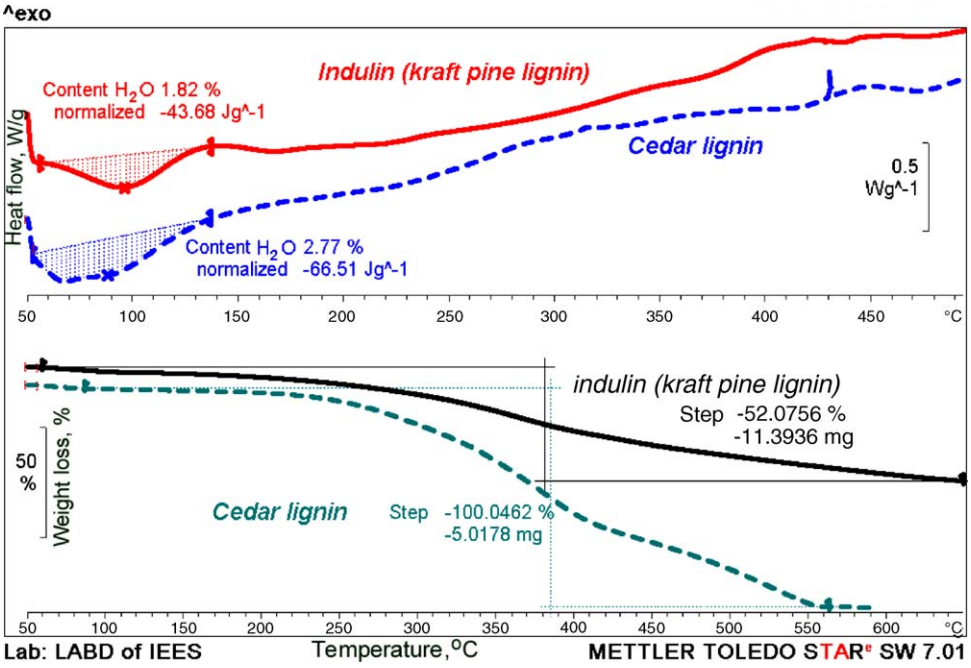

Fig. 3. DSC and TG curves for Indulin and Cedar lignin.

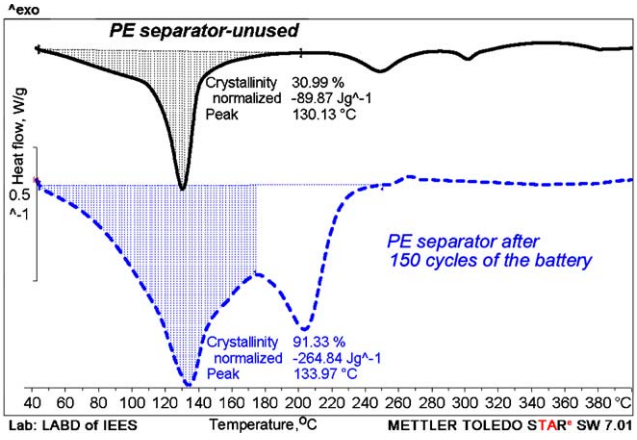

Fig. 4. DSC curves for PE separators.

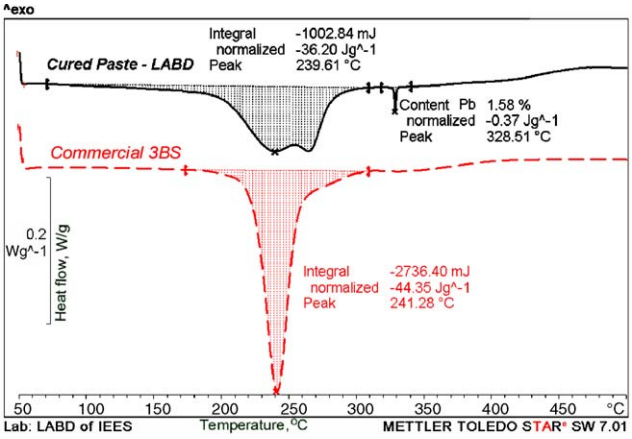

Fig. 5. DSC curves for cured positive 3BS paste and commercial 3BS.

During paste mixing, plate curing and storage before formation, the paste material reacts with atmospheric CO_2 as a result of which it gets partially carbonated. When the percentage of the carbonates in the paste exceeds 12–15%, the battery parameters decline. Fig. 6a shows DSC curves for lead hydrocarbonate, fresh 3BS paste and 3BS paste left in humid CO_2 atmosphere for 3 h.

The endothermic peaks at 250 and 260 °C correspond to lead hydrocarbonate dehydration and that at 370 °C is related to its decomposition. The curve for the carbonated cured paste features, beside the 3BS peaks at 240 and 270 °C, two new peaks at 340 and 390 °C, which result from the degradation of the hydrocarbonate formed in the paste. The degree of carbonation can be easily determined from the TG curves shown in Fig. 6b. From these curves, we calculated that the content of hydrocarbonate formed in the paste was 1.93% of the sample weight. The use of thermal methods allows determination of the degree of paste carbonation.

3.5. 4BS pastes

Fig. 7a presents DSC curves for commercial 4BS product and for 4BS positive cured pastes. The endothermic peak at 231 °C for commercial 4BS substance and the peaks at 240 °C and at 250 °C for the cured pastes correspond to the dehydration of the traces of 3BS in the samples. 3BS, tet-PbO and orto-PbO take part in the formation of 4BS [5]. During plate curing and storage before formation, the paste material reacts with atmospheric CO_2, which results in its partial carbonation. This is illustrated by the profile of the DSC curves for the cured pastes. Additionally, two broad endothermic peaks are observed in the DSC curves along with a sharp endothermic peak due to metallic lead melting at 328 °C. The two overlapping peaks at 150–300 °C

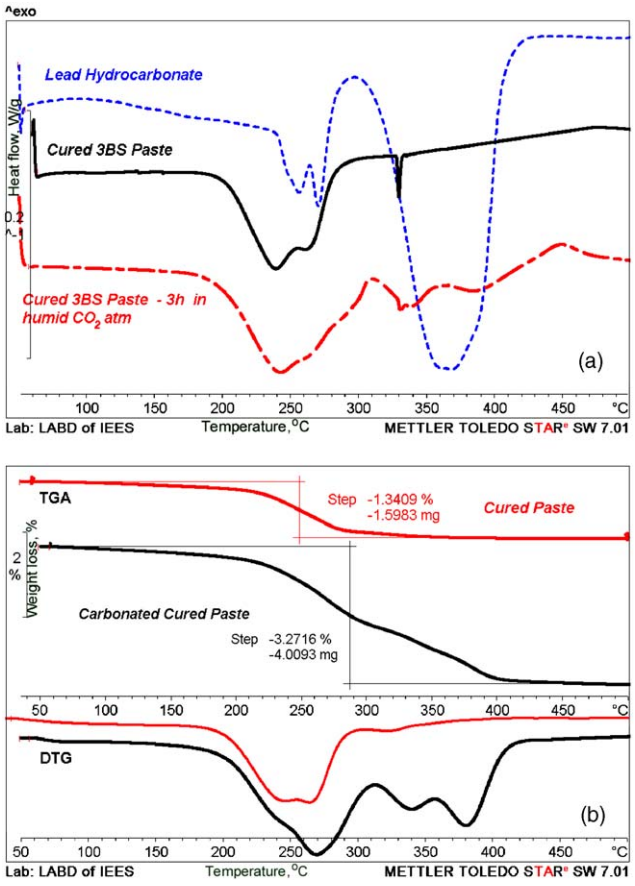

Fig. 6. DSC (a) and TGA (b) curves for fresh and carbonated cured positive pastes.

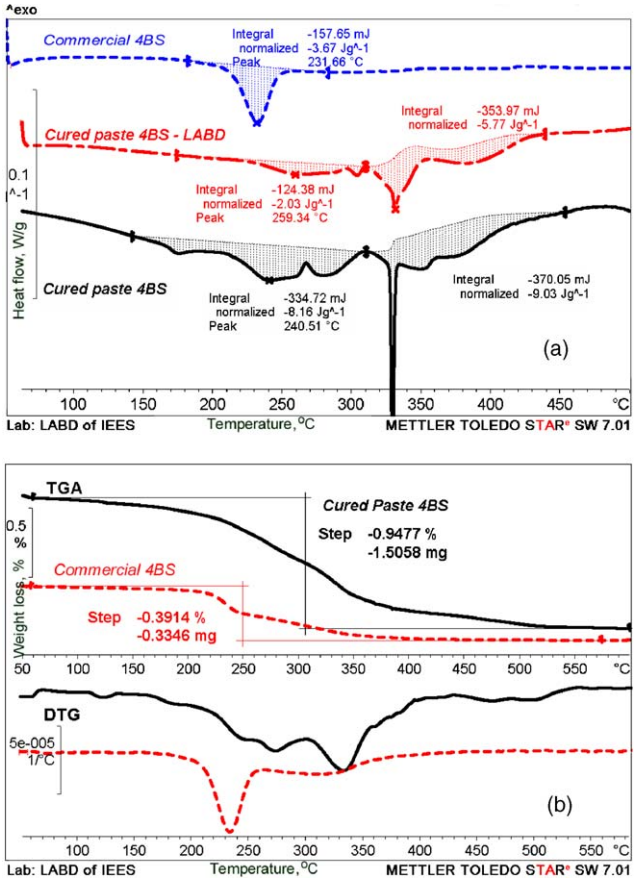

Fig. 7. DSC (a) and TGA (b) curves for commercial 4BS and cured 4BS positive pastes.

are related to the dehydration of the pastes and of hydrocarbonate in the pastes, and the peaks at 350 °C and above—to the disintegration of lead hydrocarbonate.

Fig. 7b presents TGA and DTG curves for commercial 4BS product and for 4BS positive cured paste. The cured paste looses weight in three steps: as a result of dehydration at about 240 and 270 °C, and due to the destruction of hydrocarbonates at 340 °C and above that temperature. The weight loss of the cured paste is 0.95% within the whole range of temperatures from 100 to 500 °C, i.e. it is quite small. These results indicate that the sensitivity of the method is fairly high and it can register the various types of bonding of H_2O and CO_2 in the paste.

3.6. DSC for soaked 3BS pastes

During soaking of the 3BS-pasted plates before their formation, H_2SO_4 reacts with 3BS and PbO forming $PbSO_4$. The progress of the sulphation process in the cured 3BS pastes across the plate thickness can be tracked by the changes in the area of the 3BS endothermic peaks. Fig. 8 presents DSC results for samples taken from the three sub-layers across the plate thickness after 1 h of soaking in two different solutions of sulfuric acid density: 1.06 s.g. H_2SO_4 and 1.25 s.g. H_2SO_4 [6]. From the values of the dehydration energy for the three sub-layers of the paste in 1.06 s.g. H_2SO_4 (Fig. 8a), the following distribution of the paste sulphation throughout the cross-section of the plate can be determined: 45.9% sulphation of the outer layer, 34.9% of the middle layer and 10.5% of the inner layer. Probably, in the inner layer, only the surface of the crystals forming the largest pores in the cured paste is sulphated. In the middle layer, sulphation affects also the crystals forming pores of medium radii, whereas in the outer layer some of the crystals forming smaller pores, too, are sulphated, which results in sulphation of half of the paste.

Fig. 8b shows the distribution of sulphation by paste layers: 92.0% sulphation of the outer layer, 88.8% of the middle layer and 52.5% of inner layer. These results indicate that the 1.25 s.g. H_2SO_4 has changed completely the structure and composition of the outer and middle layers of the paste for 1 h of soaking. The plate interior contains less than 50% of unreacted 3BS paste. The DSC method is an easy method to determine the sulphation processes during the soaking step of the battery manufacturing technology.

3.7. Thermal analysis of PbO_2

3.7.1. DSC results for commercial PbO_2 and PbO_2 active mass

Fig. 9 presents DSC curves for two commercial chemically produced β-PbO_2 products from different suppliers, as well as

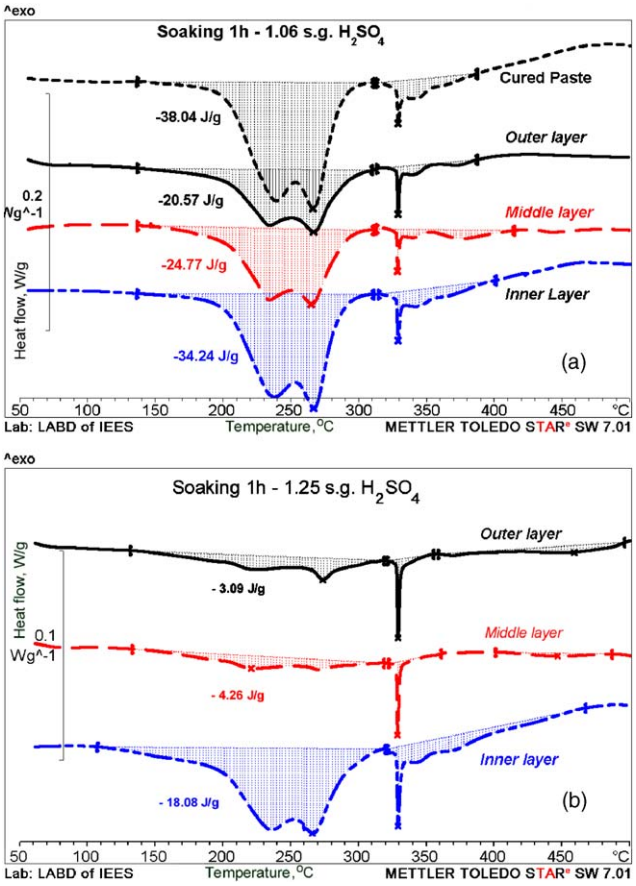

Fig. 8. DSC curves for samples taken from the three sub-layers across the plate thickness after 1 h of soaking in 1.06 s.g. H_2SO_4 (a) and in 1.25 s.g. H_2SO_4 (b).

for positive active mass (PAM) samples taken from the plates immediately after formation and after the end of battery life. The curves vary depending on the method of production and treatment of the β-PbO_2. This illustrates the high sensitivity of the DSC method to the structural changes in β-PbO_2. The curve for chemically prepared β-PbO_2 from supplier 1 features endothermic peaks at 410, 440, 470 and 490 °C, whereas in the curve for β-PbO_2 from supplier 2 the endothermic peak at 440 °C is the highest one, followed by the peaks at 470 and 490 °C.

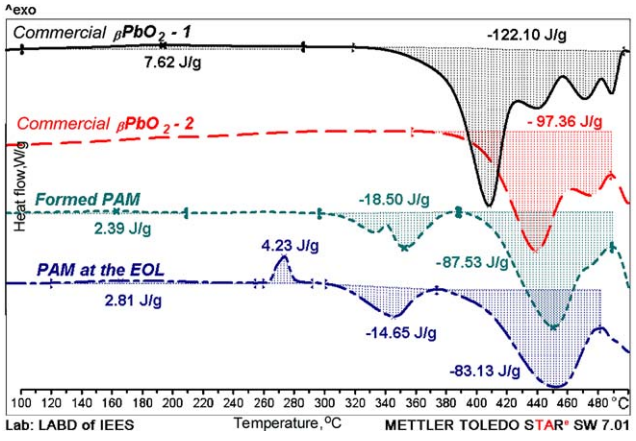

Fig. 9. DSC curves for different types of PbO_2.

It can be assumed that the peaks for β-PbO_2 from supplier 2 shift to higher temperatures (by some 30 °C). As the analytical instrument used limits the thermal measurements to 500 °C, the two high-temperature peaks cannot be registered.

The electrochemically prepared β-PbO_2 gives a small endothermic peak at 350 °C, which reflects the dehydration of $PbO(OH)_2$ or H_2PbO_3, and a second wider peak at 450 °C, which results from the decomposition of the PbO_2 to non-stoichiometric PbO_n ($1 < n < 2$). The curve for formed PbO_2 features a small endothermic peak at 490 °C (similar to that of chemically produced PbO_2 from supplier 2). The highest endothermic peak of PbO_2 decomposition tends to shift from 410 °C (β-PbO_2 from supplier 1) to 440 °C for β-PbO_2 from supplier 2 and 450 °C for electrochemically formed β-PbO_2 from the 3BS paste. The latter peak is very wide. The curve for formed PbO_2 contains an endothermic peak at temperatures higher than 500 °C. Hence, the electrochemically obtained β-PbO_2 decomposes at higher temperatures than the chemically produced oxide and contains some hydrated part, which is responsible for the wide but low peak at 350 °C. Probably, that is the reason why the formed β-PbO_2 active mass is electrochemically active, unlike the chemically produced β-PbO_2, which has no electrochemical activity [7,8]. There is still another exothermic peak at 270 °C in the DSC curve for the PAM at the end of battery life.

3.7.2. DSC analysis of PbO_2 processed at different heating rates

Fig. 10 presents DSC curves at two different heating rates for a commercial chemically produced lead dioxide product, as well as for positive active mass (PAM). Changing the heating rate, influences both the peak height and width. It can be seen from Fig. 10a and b that the curves for heating rate 10 K min^{-1} feature two larger endothermic peaks shifted to higher temperatures. Hence, we can amplify minor effects by applying higher heating rates. The sensitivity increases with increasing the heating rate. For the peak separation, a low heating rate is necessary. We can improve the resolution by decreasing the heating rate. The curves obtained at lower heating rate, 2 K min^{-1}, feature three smaller endothermic peaks shifted to the lower temperatures. At high heating rates, the reactions of decomposition of β-PbO_2 cannot proceed fully. That is the reason for the different normalized energy values of the endothermic peaks registered at different heating rates.

3.7.3. DSC and TGA curves for samples from different PAM sub-layers of the plate

Fig. 11 presents the thermal spectra for lead dioxide positive active mass samples (PAM) from a tubular plate. The samples are taken from one electrode at different distances from the current collector situated in the middle of the tube. The area of endothermic peak at 455 °C, which is related to β-PbO_2 decomposition, decreases slowly on approaching to the current collector. The curve for the sample of the layer 2 in the bulk of PAM features three overlapping peaks. The peak at 350 °C reflects the evaporation of the hydrated water, a second small endothermic peak at 380 °C (in white) and a wider peak at 455 °C result from the decomposition of PbO_2 to non-stoichiometric oxides. The

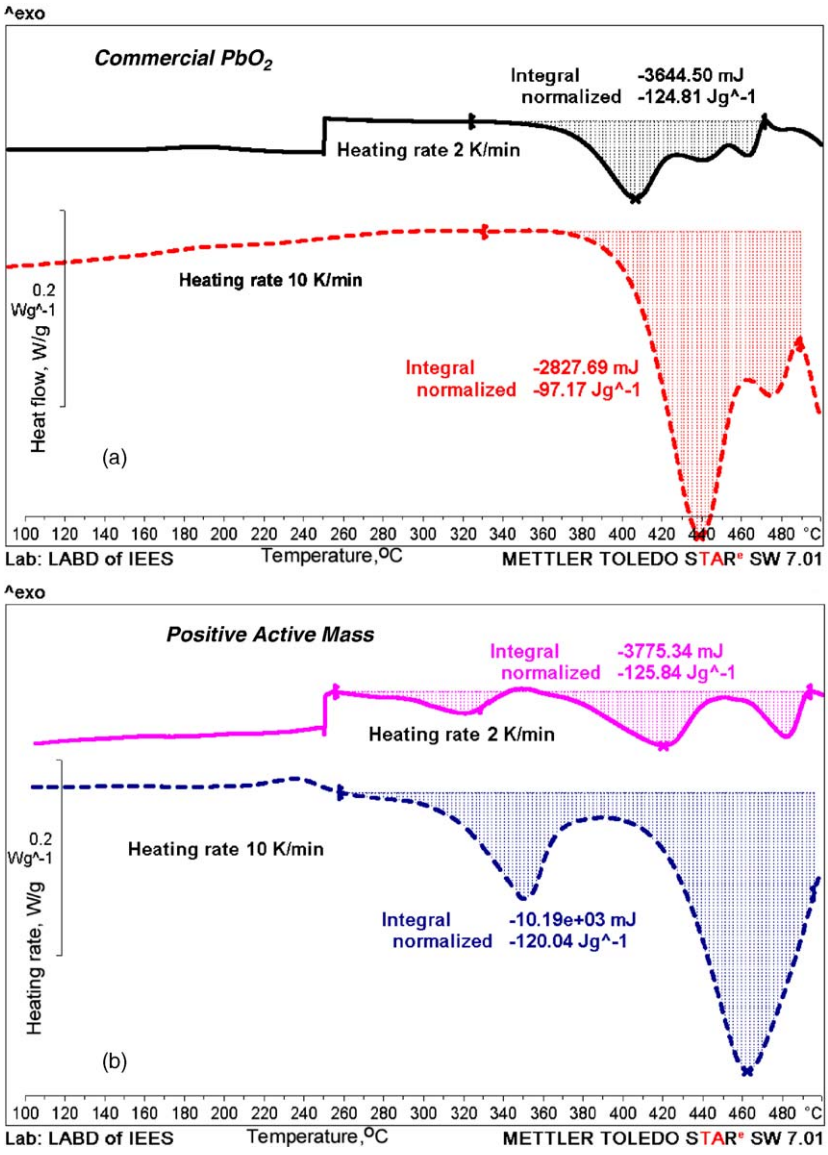

Fig. 10. DSC curves for commercial PbO_2 (a) and for positive active mass (b) at heating rates 10 and 2 K min^{-1}.

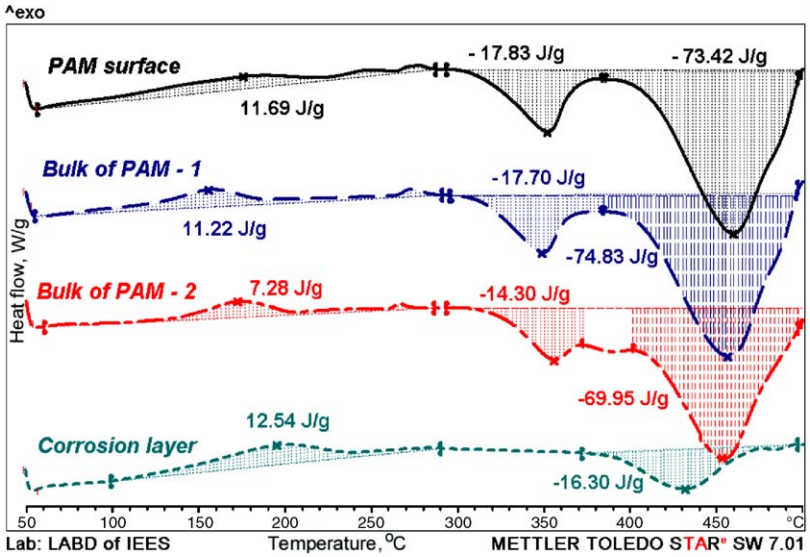

Fig. 11. DSC curves for different types of positive active masses.

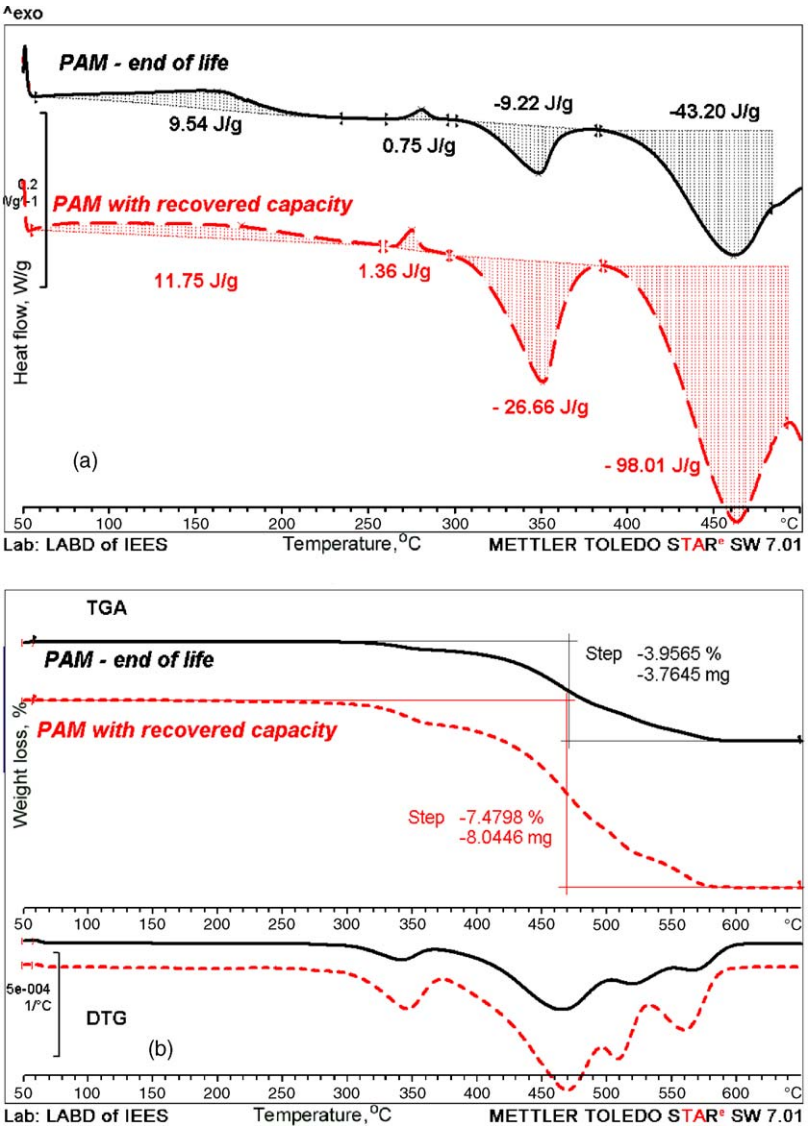

Fig. 12. DSC (a) and TGA (b) curves for positive active mass with declined capacity and for positive active mass with recovered capacity.

profile of the curve for the corrosion layer changes completely, which is an indication of phase composition changes.

3.7.4. DSC and TGA of PAM with declined capacity and after capacity recovery

Positive active mass (PAM) degradation proceeds in two ways: reversible and irreversible. If a battery whose capacity has declined is subjected to capacity recovery cycles, the rated capacity is restored and the battery can be used further. No substantial differences can be seen in the phase composition and microstructure of PAM with recovered capacity and PAM at the end of battery life through X-ray diffraction analysis and SEM observations. Fig. 12a presents the DSC curves for PAM from a battery at its end of life and PAM from a plate with recovered capacity.

The energies of the peaks for the positive active mass with recovered capacity are three-fold higher (for the peak at 350 °C) and twice higher (for the peak at 460 °C) than those for the positive active mass with declined capacity.

From the TGA curves, Fig. 12b, we can easily determine the degree of hydration and the steps of decomposition of the samples. The total weight loss for the sample from PAM with recovered capacity is 7.48% and it is twice higher than that for PAM at the end of battery life, 3.96%. Hence, the weight loss can provide information for the capacity of the positive active mass.

4. Conclusions

DSC and TGA are efficient analytical methods for analysis of the basic materials, sub-products and active materials for lead-acid batteries. DSC and TGA data can throw light on some of the processes taking place during battery production and operation. Thermal analytical methods give new additional information about the changes in phase composition and physical properties of the active materials. DSC and TGA are fast analytical tools requiring no pretreatment of the samples.

References

[1] www.iupak.org/publications/analytical compendium.
[2] G. Liptay, Thermochim. Acta 14 (1976) 279.
[3] G.L. Corino, R.J. Hill, A.M. Jessel, D.A.J. Rand, J.A. Wunderlich, J. Power Sources 16 (1985) 141.
[4] I. Mawston, P. Buchanan, G. Wright, J. Power Sources 48 (1995) 77.
[5] V. Iliev, D. Pavlov, J. Appl. Electrochem. 9 (1979) 555.
[6] M. Dimitrov, D. Pavlov, T. Rogachev, M. Matrakova, L. Bogdanova, J. Power Sources 140 (2005) 168.
[7] D. Pavlov, I. Balkanov, T. Halachev, P. Rachev, J. Electrochem. Soc 136 (1989) 3189.
[8] D. Pavlov, J. Electrochem. Soc. 139 (1992) 3075.